Covalent Modification of Amino Acids and Peptides Induced by Ionizing Radiation from an Electron Beam Linear Accelerator Used in Radiotherapy

Authors: Benjamin B. Minkoff, Steven T. Bruckbauer, Grzegorz Sabat, Michael M. Cox, and Michael R. Sussman

Source: Radiation Research, 191(5) : 447-459

Published By: Radiation Research Society

URL: https://doi.org/10.1667/RR15288.1

RADIATION RESEARCH **191**, 447–459 (2019)
0033-7587/19 $15.00

DOI: 10.1667/RR15288.1

Covalent Modification of Amino Acids and Peptides Induced by Ionizing Radiation from an Electron Beam Linear Accelerator Used in Radiotherapy

Benjamin B. Minkoff,[a] Steven T. Bruckbauer,[b] Grzegorz Sabat,[a] Michael M. Cox[b] and Michael R. Sussman[a,1]

[a] *Biotechnology Center and* [b] *Department of Biochemistry, University of Wisconsin-Madison, Madison, Wisconsin 53706*

Minkoff, B. B., Bruckbauer, S. T., Sabat, G., Cox, M. M. and Sussman, M. R. Covalent Modification of Amino Acids and Peptides Induced by Ionizing Radiation from an Electron Beam Linear Accelerator Used in Radiotherapy. *Radiat. Res.* 191, 447–459 (2019).

To identify modifications to amino acids that are directly induced by ionizing radiation, free amino acids and 3-residue peptides were irradiated using a linear accelerator (Linac) radiotherapy device. Mass spectrometry was performed to detail the relative sensitivity to radiation as well as identify covalent, radiation-dependent adducts. The order of reactivity of the 20 common amino acids was generally in agreement with published literature except for His (most reactive of the 20) and Cys (less reactive). Novel and previously identified modifications on the free amino acids were detected. Amino acids were far less reactive when flanked by glycine residues in a tripeptide. Order of reactivity, with GVG most and GEG least, was substantially altered, as were patterns of modification. Radiation reactivity of amino acids is clearly and strongly affected by conversion of the α-amino and α-carboxyl groups to peptide bonds, and the presence of neighboring amino acid residues.

INTRODUCTION

Biological systems have evolved multiple mechanisms to combat oxidative damage induced by free radicals (*1–8*). Acute exposure to ionizing radiation produces higher levels of reactive oxygen species than most organisms can ameliorate, although tolerance varies significantly among organisms. For example, a dose of <10 Gy is lethal to humans (*9*), whereas the radiation-resistant bacterium *Deinococcus radiodurans* can survive doses in excess of 10,000 Gy (*2*). All cellular macromolecules are targets of radiation-generated free radicals. The *in vivo* effect on the genome and transcriptome (e.g., DNA or RNA strand breakage) is substantial (*10*). However, the proteome may be the primary target of free radicals due to protein abundance and reactivity (*11, 12*).

In aqueous systems, radiation treatment produces many reactive species, including solvated free electrons (e_{aq}^-), hydroxyl radicals ($OH^\bullet$), superoxides (O_2^-), hydroperoxyls ($HO_2^\bullet$) and hydrogen peroxide (H_2O_2). The effects of these species on free amino acids in solution have been studied using synchrotron-generated X rays or elemental decay-generated gamma rays (*13–17*). Major products of exposure to radiation involve classical oxidation, such as +16 (oxidation/hydroxylation; $–CH_2^- \rightarrow –CH–OH$) and +14 (carbonylation; $–CH_2^- \rightarrow C{=}O$) (*13–15*). Other products have been noted as well, such as side chain ring opening or isobaric conversion between amino acids via loss of side chain groups (*17*). In addition, rate constants have been established for the reaction of e_{aq}^- and $OH^\bullet$ with amino acids (*18, 19*). Relative reactivities of common amino acids, encompassing many possible products, have also been empirically determined by monitoring the loss of the unmodified amino acid reactant using mass spectrometry (*17, 20*).

The effects of radiation on particular amino acids have been examined within a peptide context as well. In general, the peptides used have contained sequences of biological interest or have focused on specific chemistries (*16, 17, 21–24*). In a study by Morgan *et al*. (*24*), peptides containing Gly/Ala/Val/Pro residues were used to examine a reported preference for these residues in radical-dependent peptide cleavage. In their published study, Saludino *et al*. examined the effect of aliphatic side group radicals within a tripeptide context as a source of proximal oxidation (*23*). In their published work, Xu *et al*. have broadly defined acidic, basic, and sulfur-containing side chain chemistries after irradiation in a variety of peptide contexts (*16, 21, 22*). To build on and expand this base, we now provide a comprehensive comparison of relative sensitivity to radiation and modifications among all 20 of the common amino acids free in solution or within a standardized tripeptide context.

The effect of radiation on amino acid chemistry is highly relevant to fields ranging from cancer radiotherapy to space

Editor's note. The online version of this article (DOI: 10.1667/RR15288.1) contains supplementary information that is available to all authorized users.

[1] Address for correspondence: University of Wisconsin-Madison, Biochemistry and Biotechnology Center, 425 Henry Mall, Madison, WI 53706; email address: msussman@wisc.edu.

travel to national defense (*25–29*). The first step in detailing these chemistries is to bridge the gaps in our understanding of the differences between radiation effects on free amino acids and amino acids participating in peptide bonds. Towards that end, we have used mass spectrometry to empirically analyze relative sensitivity to radiation and modifications induced by radiation for both free amino acids and amino acids in tripeptides. This work makes use of a clinical linear accelerator (Linac) commonly used in tumor radiotherapy. The Linac-produced electron beam is maintained by the University of Wisconsin (UW)-Madison Medical Radiation Research Center (Madison, WI), which provides a highly controlled and reproducible source of radiation for building a strong foundational understanding of radiation-induced amino acid modification (*30*).

MATERIALS AND METHODS

Linac Irradiation Protocol

Stocks of amino acids were made at a concentration of 500 μ*M* in 10 ml dH_2O. Stocks were kept at –20°C and thawed when necessary. The 500-μ*M* amino acid stocks were diluted 1:10 in 1 ml total dH_2O in 1.8-ml Eppendorf tubes for each sample to be irradiated. The remaining volume in each tube was comprised of air. Stocks of tripeptides were made at a standard concentration of 10 mg/ml, and diluted to 50 μ*M* using dH_2O immediately prior to irradiation. Samples were maintained at 4°C and taken to a Varian 21EX Linac for irradiation (~15 min duration each way). For each irradiation, the Linac was set to deliver a beam of electrons with 6 MeV of energy to uniformly irradiate all samples (a total of 14) at once. To accomplish this, a special high-dose total-skin electron mode ($HDTSe^-$) was utilized, which resulted in a dose rate to the samples of approximately 72 Gy/min.

The sample tubes were placed horizontally and submerged at a depth of 1.3 cm (measured to the center of the tube's volume) in an ice-water-filled plastic tank and set to a source-to-surface distance (SSD) of 61.7 cm. A 30×30 cm^2 square-field size was set at the Linac console, which gave an effective field size at this SSD of 18.5×18.5 cm^2. This is ample coverage to provide a uniform dose to all of the 1.5-ml sample tubes. The monitor unit calculations (determination of the amount of time to leave the Linac on) were based on the American Association of Physicists in Medicine (AAPM) Task Group 51 protocol for reference dosimetry (*62*). This is the standard method for determining dose per monitor unit in water for radiation therapy calculations. Once the dose was determined in the AAPM Task Group 51 reference protocol conditions (SSD = 100 cm and depth = 10 cm), an ion chamber and water-equivalent plastic slabs were used to translate this dose to the specific conditions used in this project. Irradiation was performed while the samples remained submerged at a depth of 1.3 cm in water. After irradiation, samples were frozen at –20°C until needed. The following amino acids were used: L-Isoleucine, L-Proline and the remaining amino acids came from a L-amino acids kit (all from (Sigma-Aldrich® LLC, St. Louis, MO).

High-Resolution Liquid Chromatography/Electrospray Ionization Time-of-Flight Mass Spectrometry (LC/ESI-TOF-MS) Analysis of Amino Acids

LC/ESI-TOF-MS analysis of radiation-dosed amino acids in water was performed using a liquid chromatograph/mass selective detector time (LC/MSD TOF) Agilent system equipped with a 1200 series HPLC liquid handling system (Agilent Technologies Inc., Palo Alto, CA). Compounds were measured under positive- or negative-ion polarity, whereby 2 μl of control or irradiated sample was injected from an autosampler vial sitting at 6°C into an isocratic 0.05 ml/min flow of 50:50 (water/0.1% formic acid):(acetonitrile/0.1% formic acid). The following instrumental parameters were used to generate the most optimum protonated ($M+H^+$) or deprotonated ($M-H^-$) ions under their respective acquisition polarity: Capillary voltage (3,000 V); drying gas (7 l/min); gas temperature (300°C); nebulizer (15 psig); oct DC1 (35 V) for positive and (–34 V) for negative ionization; fragmentor (140 V); oct RF (200 V); skimmer (60 V). Internal calibration was achieved with assisted spray of two reference masses, 112.9856 m/z and 1033.9881 m/z. Data were acquired in profile mode scanning from 50–1,600 AMU at 0.89 cycles per s and 10,000 transients per scan.

Liquid Chromatography-Assisted Ultra-High-Resolution Electrospray Ionization (LC-UHR-ES) Orbitrap Mass Spectrometry Analysis of Tripeptides

LC-UHR-ESI-Orbitrap analysis of irradiated tripeptides in water was done on Thermo Scientific LTQ-Orbitrap Elite™ system equipped with an Ion Max electrospray source. Compounds were measured under positive ion polarity in profile mode either as a one-scan or five-scan event, where 2 μl of control or irradiated sample was injected from an autosampler vial sitting at 6°C into an isocratic 0.05 ml/min flow of 50:50 (water/0.1% formic acid:acetonitrile/0.1% formic acid). The one-scan event consisted of a continuous MS1 scanning at 120,000 resolution over 50–1,000 m/z mass range. The five-scan event consisted of continuous cycle of a single MS1 scan at 120,000 resolution over 50–400 m/z followed by four MS/MS scans on the four most abundant precursors observed in the preceding MS1 event. Higher energy collisional (HCD)-based fragmentation with a normalized collision energy of 35% and isolation width of 1.2 Da was scanned into the Orbitrap under 15,000 resolution. The following instrumental parameters were used to generate the most optimum protonated ($M+H^+$) ions: Source voltage (3,800 V); source heater (100°C); capillary temperature (320°C); sheath gas flow (15); auxiliary gas flow (5); S-lens RF level (35%); multipole RF amplifier (600).

MS Data Analysis

Data processing of the single amino acids was executed using Analyst QS version 1.1 (build: 9865) software (Agilent Technologies) to extract unique masses observed in the spectrum. This semi-manual analysis strategy was further complemented and verified with fully-automatic processing using Agilent's MassHunter Workstation Qualitative Analysis software, version B.01.03 (build: 1.3.157.0), where centroided data (filtered based on absolute peak height of 200 counts per s, minimum to differentiate peaks from the baseline on our instrument) was used to assign compounds from their molecular features and ultimately generate extracted ion abundance chromatograms (using original profile data) to aid in quantification and distribution over the entire radiation dosage spectrum.

Data processing of the tripeptides was executed using the Xcalibur™ Qual Browser (Thermo Fisher Scientific™ Inc., Waltham, MA). A boxcar smoothing of 7 and ppm window of 4 amu was used to extract ion chromatograms for the unmodified version of the tripeptide and all modifications observed. Modifications were identified by examining spectra averaged over the injection curve per sample, with a S/N threshold of >1.0% for peak identification. Whether the 1+ or the 2+ variant of the tripeptide was used for quantification is specified in Supplementary Table S1 (http://dx.doi.org/10.1667/RR15288.1.S1), when both forms were identified. Area under extracted ion chromatograms was calculated using Qual Browser's automatic peak picking algorithm.

Relative reactivity rates were calculated by fitting linear trendlines to the obtained data as specified. For the amino acids, the doses used included 0, 100 and 200 Gy. For tripeptides, radiation doses across the full range (0–1,000 Gy) were used. No fitting was performed for

modification appearance rates. Tripeptide volumes were determined using the online tool, Peptide Property Calculator (https://bit.ly/2IkH9yY) (*53*).

RESULTS

Overview of Experimental Design and Rationale

Free amino acids in solution were first analyzed via mass spectrometry after irradiation at a range of doses using the Linac. Relative sensitivity to radiation and dose-dependent product formation were documented. Next, tripeptides were synthesized with the composition G-X-G, where every amino acid was separately placed in the X position. Glycine was chosen because it is relatively nonreactive compared to the remaining 19 amino acids free in solution. With the amino acids thus placed in a more protein-relevant context, we both determined radiation sensitivity and identified covalent modifications on the tripeptides using mass spectrometry. A goal of this work was to catalog the modifications induced by UW-Madison's radiation source for this and future studies and provide a benchmark comparison with other previously reported reactivities of amino acids with radiation-generated radicals.

Radiation Response and Modification of Free Amino Acids in Aqueous Solution

To begin with the simplest possible system, 50-μ*M* solutions were made of each of the common 20 amino acids in water. Each solution was irradiated with 0, 100, 200, 500 or 1,000 Gy. The products were analyzed using ESI-TOF mass spectrometry with both positive and negative mode (Supplementary Table S2; http://dx.doi.org/10.1667/RR15288.1.S2), and the loss of the unmodified form of the amino acids was monitored. This is shown here as a percentage of the control signal per amino acid remaining after each dose of radiation (Fig. 1A).

For the majority of amino acids, a significant portion of signal from the unmodified forms was lost after the 200 Gy dose, suggesting their complete conversion to products at or before the subsequent 500 Gy dose (Fig. 1A). For the majority of amino acids with unmodified signal remaining after receiving the 200 Gy dose, the linear rate of loss displayed from 0 to 200 Gy then slowed significantly for higher doses. Concurrent with this, increased production of many modifications was lost after exposure to 200 Gy (Supplementary Figs. S1–S3; http://dx.doi.org/10.1667/RR15288.1.S5). Furthermore, in the cases where modification signals still increased beyond the 200 Gy dose, the rate was significantly slower (Supplementary Figs. S1–S3). Thus, linear relative rates of dose response, corresponding to their respective radiation sensitivities, were built using the data from 0 to 200 Gy for each amino acid, and plotted over this range (Fig. 1B, based on data from Supplementary Table S2; http://dx.doi.org/10.1667/RR15288.1.S2). Using these relative sensitivities, a scale of response was constructed and compared to published data from other ROS-producing techniques (*17, 18, 31*) (Fig. 1C). The most sensitive amino acid was His. Relative to previously published studies (*16, 17, 31*), the significant response of His observed here is unusual and may be specific to the high-energy electron beam used. Otherwise, the relative amino acid dose responses are generally consistent with previously reported data (*17*).

Correlations of sensitivity with side group chemistries and physicochemical properties of amino acids, including volume (*32*), hydropathy (*33*) and pKa/pI values, were calculated (Supplementary Figs. S4 and S5; http://dx.doi.org/10.1667/RR15288.1.S5). The response of the amino acids containing aromatic R groups produced the most notable grouping (Fig. 1D). The strongest correlation of radiosensitivity level with a physicochemical property was with molecular volume ($R^2 = 0.5672$; Supplementary Fig. S5), suggesting there may be some dependence on volume for the relative sensitivities to radiation we observe. The aromatic ring-containing residues were all highly responsive, and exhibited similar dose responses of modification (Fig. 1D). They also all exhibited multiple oxidation events (Fig. 1E and Supplementary Fig. S6; http://dx.doi.org/10.1667/RR15288.1.S5), which we hypothesize to be due to resonance associated with the aromatic rings. No other significant correlations between responses or modifications and chemical properties of amino acids were observed (Supplementary Figs. S4 and S5).

Classical hydroxylation (+16)(+O) was observed on each amino acid except for Asp, Cys and Gly (Table 1). Dihydroxylation/peroxidation (+32)(+2O) events were seen on the vast majority of amino acids. Carbonylation (+14) was observed on less than one half of the amino acids. For His, Lys and Cys only, adducts of +48 were observed (Table 1 and Supplementary Table S2; http://dx.doi.org/10.1667/RR15288.1.S2). This is likely a combination of +16 hydroxyl and +32 dihydroxyl/peroxy product mass shifts. A generalized reaction scheme for these common oxidative modifications is shown in Fig. 2.

With radiation treatment, a number of products of very low signal with less mass than the unmodified amino acid were observed for the majority of amino acids (Supplementary Table S2; http://dx.doi.org/10.1667/RR15288.1.S2). Despite the abundance of many products, including classical oxidation and others with known atomic composition, there was not a strong correlation between the disappearance of unmodified amino acid variants (orders of magnitude) and the appearance of particular products. Thus, the reaction pathways leading to products caused by radiation are likely to be complex, an issue that must be addressed in future work.

Modifications of Aromatic Amino Acids in Solution

The aromatic ring-containing residues were the most highly modified subset of amino acids. Each was signifi-

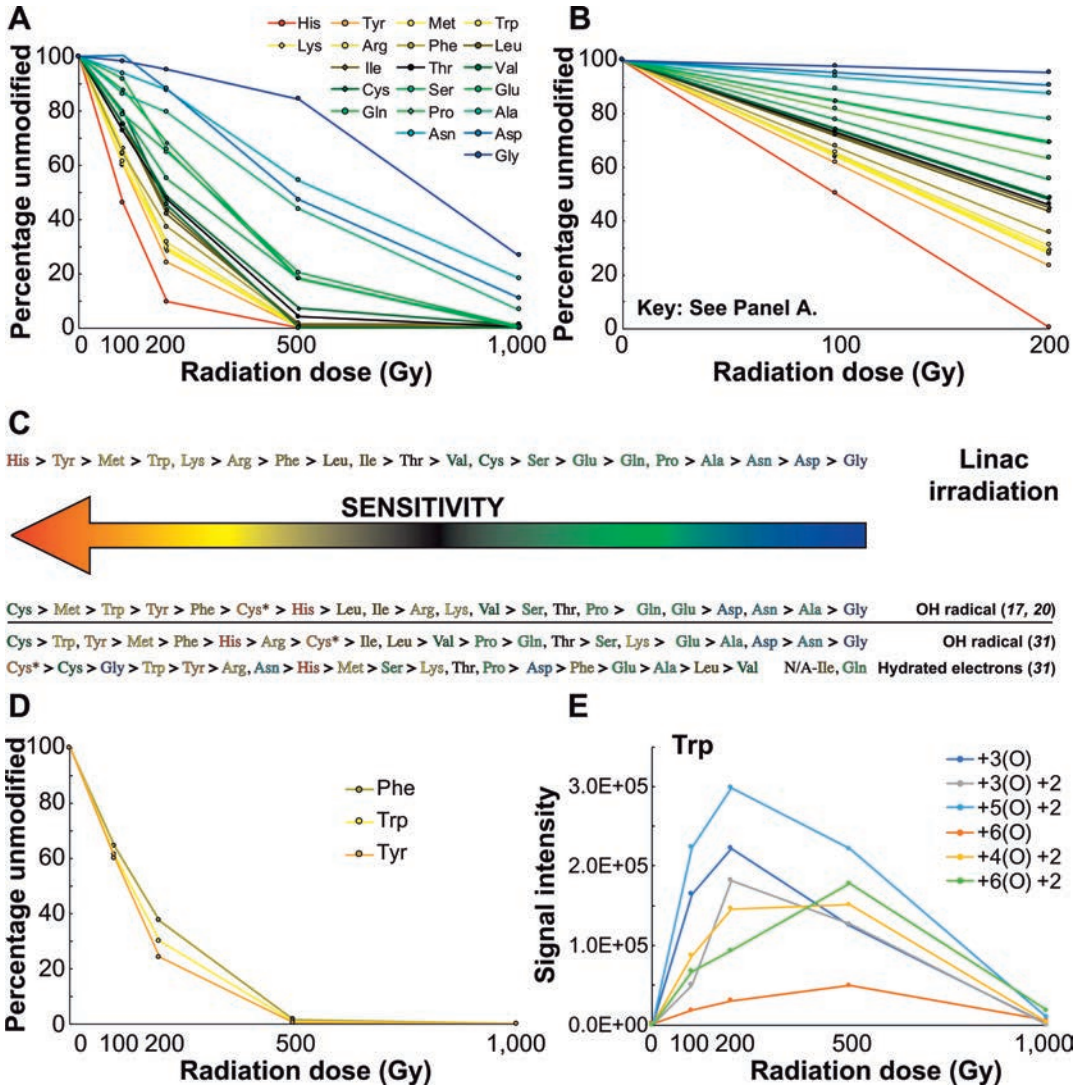

FIG. 1. Panel A: Raw signal loss for unmodified amino acids at 50 μ*M* in H_2O. Panel B: Linearization from 0 to 200 Gy, the linear range of reactant loss. Panel C: Relative reactivities of amino acids charted altogether and compared to reactivities determined using techniques reported elsewhere (*17, 20, 31*). Panel D: The cluster of aromatic ring-containing residues. Panel E: Modification events identified and their abundance on Tyr, from ESI-TOF MS.

cantly modified with +16n adducts, up to n = 6 (Table 1 and Supplementary Table S2; http://dx.doi.org/10.1667/RR15288.1.S2). For Trp and Phe, higher oxidation states were observed with a 32+2 (+34) mass shift, which may be a result of a combination of di-hydroxylation of the benzene ring across a double bond (+17 each). These occurred in addition to hydroxylation elsewhere in the molecule (+16). The major products of Trp oxidation are hydroxytryptophan (+16), di-hydroxytryptophan (+32), kynurenine (+4) and oxidation or N-formylation of the kynurenine product (+20 or +32, respectively) (*15, 17, 34*). Tyr conversion to dihydroxy derivatives and subsequent dimerization was observed in work reported elsewhere (*35–37*), although this product was not observed here. Finally, Phe hydroxylation about the benzene ring to form ortho- or meta-tyrosine has been observed elsewhere (*15, 38*). However, the multiple oxidation events on all aromatic residues described above have not been previously reported (Supplementary Fig. S6; http://dx.doi.org/10.1667/RR15288.1.S5). A combination of hydroxylation (+16) and peroxidation (+32) events may explain the results of Supplementary Fig. S6, although the extent of either cannot be determined for the higher-order modifications. We hypothesize that the reactivity patterns of aromatic amino acids observed reflect the use of free amino acids in the current study, leading to some novel patterns not observed in the peptides used in the previous studies cited. Furthermore, the loci of modifications were not identified, so it is possible that hydroxylation and peroxidation are occurring throughout the molecules, rather than solely on the benzene rings.

TABLE 1
Linac Radiation-Induced Products of Free Amino Acids

		Modifications				
Amino acid	R chemistry	+16Da/+(O)	+32Da/+2(O)	+16(n)Da/+n(O)	+14Da/+(=O)	Miscellaneous
F	Aromatic	+	+	+(3–5)		+66, +82
W	Aromatic	+	+	+(3–6)		+50, +66, +82
Y	Aromatic	+	+	+(3–4)		+66
D	Acidic					–30, +137
E	Acidic	+	+		+	–30, –14
A	Nonpolar	+	+			
G	Nonpolar					
I	Nonpolar	+	+		+	
L	Nonpolar	+	+		+	
M	Nonpolar	+				–55
P	Nonpolar	+	+		+	
V	Nonpolar	+	+		+	
C	Polar			+(3)		
N	Polar	+	+			
Q	Polar	+	+		+	
S	Polar	+				–2, –28
T	Polar	+	+			–46
H	Basic	+	+	+(3)		+5, +8, +35, –10, –22, –28
K	Basic	+	+	+(3)	+	
R	Basic	+	+		+	–43, –61

Notes. Shown in columns are presence (+) of common modifications, including oxidation/hydroxylation (+16Da), peroxidation (+32Da), multiple oxidation events [+16(*n*)Da, where *n* is the number of events observed] and carbonylation (+14Da). Uncommon modifications are displayed in the ''Miscellaneous'' column, and the mass shifts, in Da, are shown for each amino acid.

Modifications of Acidic Amino Acids in Solution

Consistent with previously reported observations (*15, 22*), decarboxylation of the R-group was seen on the negatively charged amino acids Asp and Glu (Table 1, Supplementary Table S2; http://dx.doi.org/10.1667/RR15288.1.S1). On Glu, hydroxylation (+16), peroxidation (+32) and carbonylation (+14) were all seen. A –14 mass shift [(described elsewhere (*16*) as oxidative decarboxylation followed by a +16 oxidative addition] was also observed, whereas no shift was seen on Asp. However, a significant mass shift of +137 was seen on Asp, which is 5 Da heavier than a dimerized form of Asp. At this point, it cannot be determined whether this is actually a dimerized Asp product. This mass at ca. 271 m/z was present at low signal in the untreated samples, although its formation is clearly induced to some degree by radiation. Thus, it may be a change induced to different levels by both ambient radiation and aging of the powdered stock in an aerobic environment.

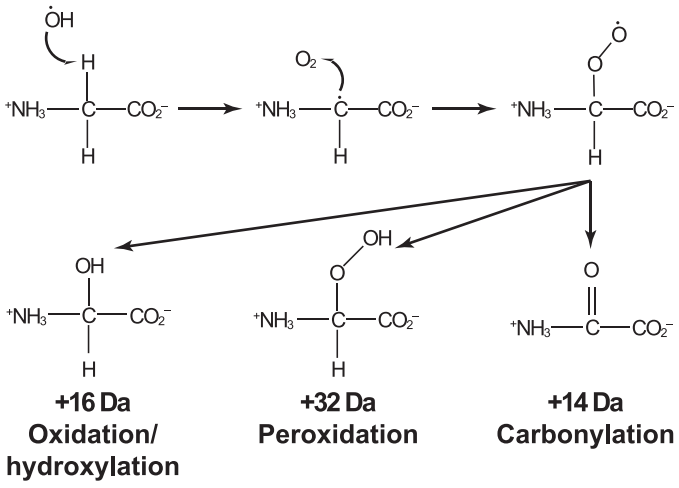

FIG. 2. Generalized reaction scheme for the most common oxidative modifications to amino acids and proteins. After hydrogen abstraction at the α-carbon, carbon or oxygen radical species can further react to produce hydroxylation (+16) , peroxidation (+32) or carbonylation (+14).

Modifications of Aliphatic/Nonpolar Amino Acids in Solution

Irradiation of hydrocarbon aliphatic/nonpolar amino acids yielded hydroxylation (+16), dihydroxylation/peroxidation (+32) and carbonylation (+14), in agreement with the published literature (Table 1 and Supplementary Table S2; http://dx.doi.org/10.1667/RR15288.1.S2) (*14, 15, 17*). Gly exhibited the lowest dose response, as observed elsewhere (*17, 19*). Given that only a fourfold loss of Gly was observed with the highest radiation dose, and no discrete product formation was observed, we hypothesize that formation of many different products below the limit of detection may be occurring. Furthermore, much of the literature suggests the major product of Gly modification with radicals occurs as backbone cleavage of polypeptides (*19, 39, 40*), which would not be observed in these data. Relative to Gly and Ala, more modification was seen on the nonpolar residues with a greater number of C-H bonds (Ile, Leu and Val), as reported elsewhere (*11*). Other minor products of the hydrocarbon aliphatic acids have been

observed under a variety of conditions, but none were found here (*31*). Modification of +16, +32 and +14 was seen on Pro. The +16 mass shift on Pro could represent either 5-hydroxyproline or glutamyl semialdehyde, as the two species are reportedly in equilibrium (*40–43*). Similarly, a mass shift of +32 corresponds to either dihydroxylation, peroxidation or conversion to Glu. The +14 product is conversion to pyroglutamic acid via carbonylation (*15, 17*).

Modifications of Polar Amino Acids in Solution

Amino acids containing polar side chains yielded a wider variety of products than those in the nonpolar group (Table 1 and Supplementary Table S2; http://dx.doi.org/10.1667/RR15288.1.S2). Asn, Gln, Ser and Thr have not been as extensively studied as the other amino acids. Hydroxylation and carbonylation have been reported for Asn and Gln, although product formation is low in signal (*16*). In addition to hydroxylation on both Asn and Gln, we observed dihydroxylation/peroxidation (+32), the first report of such, as well as carbonylation (+14) on Gln. No other Asn or Gln products were observed. Both Ser and Thr were hydroxylated (+16), whereas radiation treatment of Thr also yielded a dihydroxylation/peroxidation (+32) product. Consistent with previously published data, a mass shift of –2 was observed on Ser, corresponding to hydroxyl side chain conversion to a carbonyl group (*16*). The strongest signals were mass shifts of –28 for Ser and –46 for Thr, corresponding to the loss of CO and C_2OH_6, respectively. We hypothesize that these alterations correspond to loss of the respective side chains, via an unknown mechanism.

Modifications of Sulfur-Containing Amino Acids in Solution

In contrast to previously reported studies (*16, 17, 31*), the sulfur side chain-containing amino acids Met and Cys were not observed to be the most responsive. Whereas Met was one of the more sensitive residues, Cys was close to the middle of all of the amino acids with respect to sensitivity (Fig. 1C). We identified a mass shift of +16 on Met to form methionine sulfoxide, corresponding to the classical oxidative product, which has been previously reported many times (*16, 17, 31, 44, 45*). Sulfoxide formation is strongly induced at a radiation dose of 100 Gy, after which the signal remains stable at 200 Gy but drops significantly thereafter. In negative mode, a strong, dose-dependent signal that persisted to 1,000 Gy was observed for methanesulfonic acid (–55; Supplementary Table S2). Given the highly oxidative environment created upon irradiation, we posit this is a cleavage product of unmodified Met and methionine sulfoxide. We hypothesize that radiation triggers a quick conversion of Met to methionine sulfoxide, after which the main byproduct is methanesulfonic acid.

Cys was less sensitive than previously reported (*17, 31*) (Fig. 1A). With Cys, the major product formed is cysteine sulfonic acid, the triply oxidized Cys species (+48). This modification has been observed on the tripeptide GCG and a much longer peptide (*16*) as well as free Cys (*46, 47*). Additionally, we observed formation of cystine (Cys*), the disulfide-linked, dimeric form of Cys (Table 1 and Supplementary Table S2; http://dx.doi.org/10.1667/RR15288.1.S2). The proposed mechanism for Cys* formation is hydrogen abstraction from the sulfhydryl group followed by subsequent radical dimerization (*31, 46, 47*). The abundance of Cys* initially increases at 100 Gy dose and decreases at higher doses, presumably as other products are formed. Xu and Chance noted this phenomenon previously in experiments to irradiate a disulfide linked dipeptide $(GC)_2$. They observed free dipeptide produced via disulfide cleavage (*16*). The major product was monomeric GC-sulfonic acid, as observed here. A number of additional products, including +16 and +32, were produced from the dipeptide as reported but not observed here with the free amino acid.

Modifications of Basic Amino Acids in Solution

Finally, the basic amino acids were all among the most sensitive (Fig. 1C). Their modification profiles also follow this trend. Mass adducts up to +48 were observed on both Lys and His. Arg produced unique products, and many products of His were seen (Tables 1 and Supplementary Table S2; http://dx.doi.org/10.1667/RR15288.1.S2). Conversion of Arg to glutamic-semialdehyde (–43) has been noted multiple times, both in radiolysis and metal-catalyzed oxidation (*21, 41, 43*), and was also observed here. We also identified a –61 product of Arg, the molecular composition of which is unknown. On His, mass shifts of +5, +8, +35, –10, –22 and –28 were observed, in addition to mass shifts of +16n up to n = 3. Oxidation to form 2-oxohistidine and the –22 conversion to Asp were noted many years ago elsewhere (*48*), and the +5 and –10 products have been reported more recently (*17, 21*). Mass shifts within this dataset of +8, +35 and –28 are also present (Supplementary Table S2). While studies have been published examining oxidation pathways of His (*49–52*), none of the reported intermediates are consistent with the masses of unknown composition identified here.

Radiation Response of Amino Acids in a Peptide Context

A second goal of this study was to examine the effect of radiation on amino acids when the α-amino and α-carboxyl groups are incorporated into peptide bonds. Thus, we next turned to tripeptides. Gly, the least reactive residue, was chosen to provide the peptide linkages. This allowed us to isolate, as much as possible, the effects of the peptide bonds themselves. All 20 tripeptides were synthesized as G-X-G, where X is an amino acid. For 15 of the 20 tripeptides, radiation treatment from 100 to 1,000 Gy was performed, identical to the procedure used for the free amino acids, in water at a concentration of 50 μ*M*. Both technical (analyzing the same irradiated sample multiple times on a mass spectrometer) and experimental (re-irradiating with the

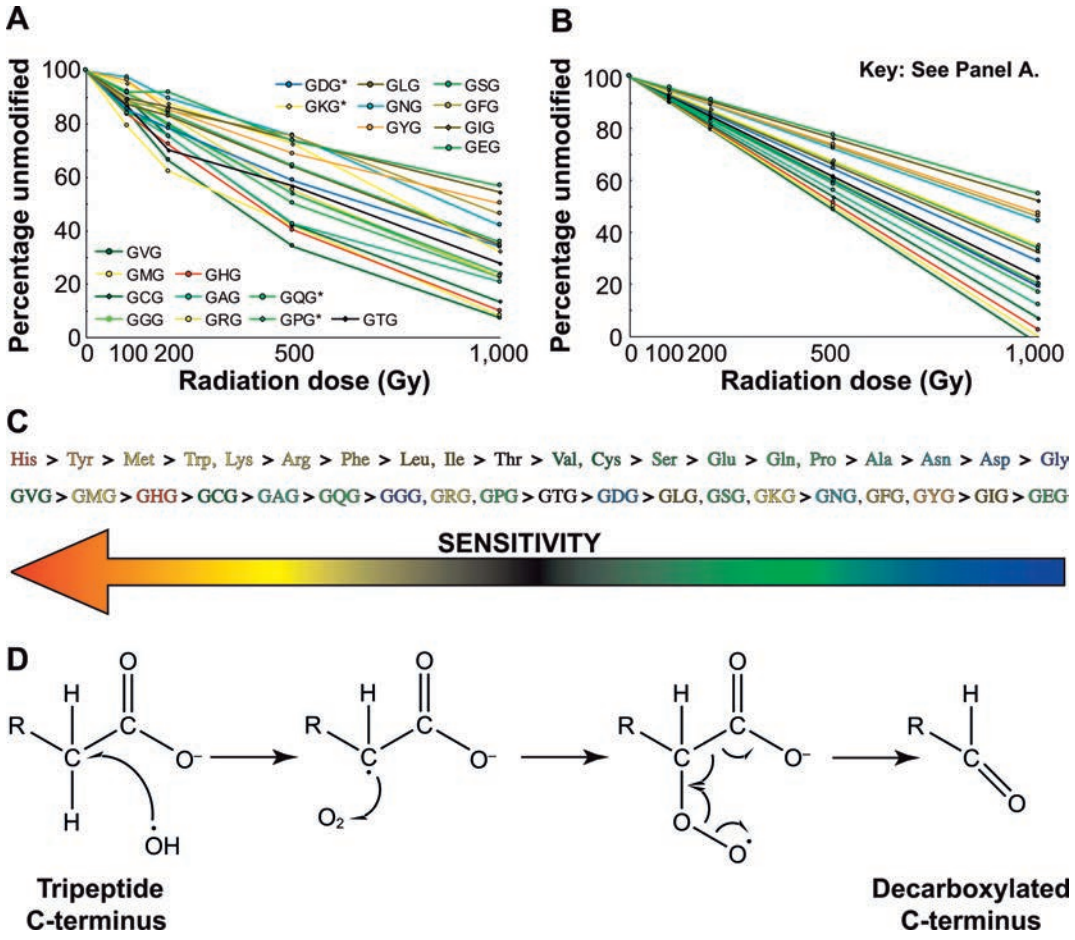

FIG. 3. Panel A: Raw signal loss for tripeptides at 50 μ*M* in H_2O. Panel B: Linearization from 0 to 1,000 Gy, the linear range of reactant loss. Panel C: Comparison of relative reactivity rates of free amino acids and tripeptides. Panel D: Reaction scheme for C-terminal decarboxylation. R represents the first and second residues, and the sidechain and C-terminus of the third Gly residues are shown in full.

same stocks and re-analyzing radiation response) variability were assayed and the irradiation results were reproducible (Supplementary Fig. S6; http://dx.doi.org/10.1667/RR15288.1.S5). The tripeptide GWG was not soluble in water, but was solubilized into DMSO which was diluted to 0.8% for irradiation (Supplementary Fig. S7). GWG is not included in the chart of rates. Finally, at a presumed concentration of 50 μ*M*, the tripeptides GPG, GKG, GQG and GDG were significantly more sensitive than any of the other tripeptides, and the appearance of their modifications followed curves resembling free amino acids, rather than the other tripeptides (data not shown). We reasoned that this was due to misreporting of their initial quantities, and repeated the treatment at different concentrations to determine which most accurately reflected the responses of the other tripeptides (Supplementary Table S3). Thus, these four tripeptides were irradiated at a tenfold higher concentration than the others, to obtain both dose response and product formation curves representative of tripeptides (Supplementary Table S1; http://dx.doi.org/10.1667/RR15288.1.S1 and Figs. S8–S10). With this caveat in mind, the rates for these four tripeptides are included alongside the other 15. However, we were able to accurately determine dose-dependent product formation for all 20 tripeptides. All of the tripeptides were subject to ESI-Orbitrap analysis in positive mode, with MS/MS fragmentation used as secondary confirmation for mass shifts (Fig. 4 and Supplementary Table S1).

Tripeptide response to radiation was considerably different from that observed with the free amino acids. After 1,000 Gy irradiation, unmodified signal remained for all of the tripeptides (Fig. 2A), indicating that they are far less sensitive to radiation than free amino acids (Fig. 1A). Reactant loss was dose-dependent throughout the range of exposures (Fig. 3A), as was product formation (Supplementary Figs. S8–S10). Thus, linear fitting to determine relative responses was performed using data across the full range of radiation doses (Fig. 3B). GVG was the most radiosensitive tripeptide, whereas GKG was among the least, inverting the relative responses seen with the free amino acids. GAG and GGG were more sensitive than GYG and GFG, again in contrast to their behavior as free amino acids. Some tripeptides behaved similarly to their amino acid counterparts. GMG, GHG and their free amino acid

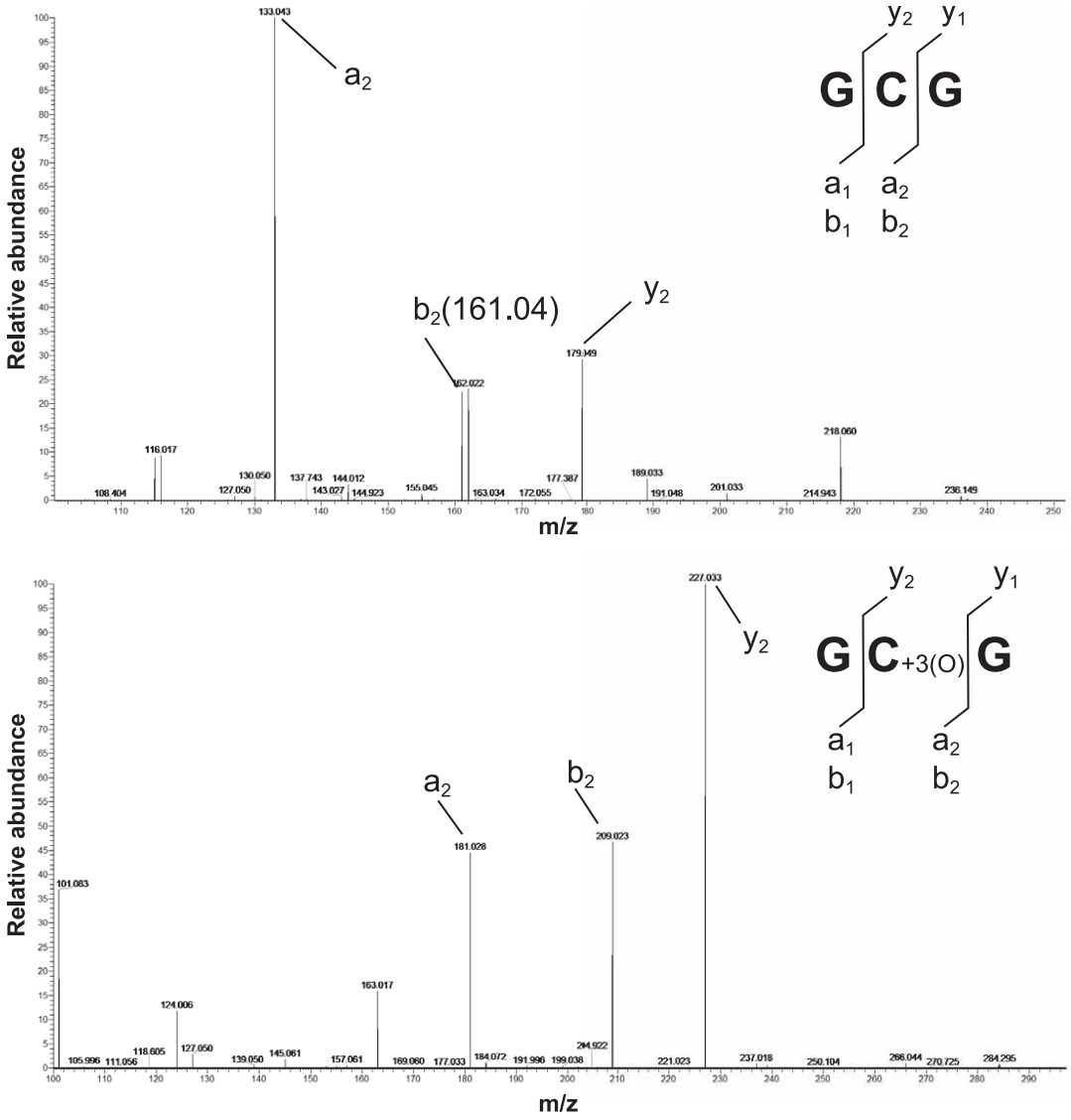

FIG. 4. Example MS/MS spectra from unmodified tripeptide GCG and triply oxidized version demonstrating fragment ion identification and localization of oxidation to middle C residue. The labels a, b, and y refer to classic fragment ion products generated by collisionally-induced dissociation within the mass spectrometer.

counterparts were among the most responsive species within their respective datasets. Similarly, the relative sensitivities of GTG and Thr were both in the middle of the order in both datasets.

The lower sensitivity of the tripeptides compared to the free amino acids contradicts the notion that a larger volume may lead to higher reactivity, a correlation observed with free amino acids (Supplementary Fig. S5; http://dx.doi.org/10.1667/RR15288.1.S5). Indeed, measuring similar correlations between molecular weight or volume (*53*) and reactivity for the tripeptides yielded nothing significant (R^2 = 0.0788 and 0.0803, respectively; Supplementary Fig. S11). The lower and tighter spread of response rates obtained for the tripeptides compared to the amino acids is also a notable result (Fig. 3B). Generally, radiation-mediated radical modification of free amino acids first involves hydrogen abstraction from or radical attack of the α-carbon (Fig. 2) (*13, 14, 17, 31, 40*). The sensitivity of a given residue in a tripeptide may thus be reduced due to steric hindrance surrounding the α-carbon by the adjacent Gly residues. Converting the α-amino and α-carboxyl groups in a free amino acid to amides may also influence the overall reaction. After the initial hydrogen abstraction, a tripeptide may have better resonance delocalization of the carbon radical intermediate than the free amino acid, leading to a longer-lived, more stable intermediate at this stage. The attachment of two Gly residues to the middle residue may explain the tighter spread of rates observed as well. Future experiments with a range of tripeptide compositions and chemistries will address these phenomena, which, to date, have not been explored.

TABLE 2
Linac Radiation-Induced Products of Tripeptides

		Modifications					
Tripeptid	R chemistry	+16Da/+(O)	+32Da/+2(O)	+48Da/+3(O)	+14Da/+(=O)	–30Da/Decarb,	Miscellaneous
GFG	Aromatic	+				+	
GWG	Aromatic	+	+	+			+62, +82
GYG	Aromatic	+				+	
GDG	Acidic	+				+	–32
GEG	Acidic					+	–105
GAG	Nonpolar					+	–105
GGG	Nonpolar	+			+	+	
GIG	Nonpolar	+			+	+	–4
GLG	Nonpolar	+			+	+	–4
GMG	Nonpolar	+					–14, –32, –50
GPG	Nonpolar	+	+		+	+	–87, –104
GVG	Nonpolar	+			+	+	–4
GCG	Polar			+			Dimer
GNG	Polar					+	–48, –105
GQG	Polar	+	+		+		–105
GSG	Polar					+	–2, –16
GTG	Polar					+	–2, –48
GHG	Basic	+	+	+			
GKG	Basic	+	+		+	+	
GRG	Basic		+		+		

Notes. Shown in columns are presence (+) of modifications, including oxidation/hydroxylation (+16Da), peroxidation (+32Da), triple oxidation (+48Da), carbonylation (+14Da) and decarboxylation (–30Da). Uncommon modifications are displayed in the ''Miscellaneous'' column, and the mass shifts, in Da, are shown for each amino acid. Dimerization of CGC is noted here as well.

Similar to the discrepancy between the radiation sensitivities observed for free amino acids and amino acids in tripeptides, patterns of modification were also different. By far, the most common product was decarboxylation (–30) of the C-terminus (Fig. 3D), which has been noted before in radiolytic modification studies with peptides of varying lengths and chemistries (*16, 21, 22*). Hydroxylation (+16) was observed on a subset of the tripeptides with aromatic and nonpolar side chain chemistries, a clear cluster of products. Carbonylation (+14) occurred mainly on the tripeptides with nonpolar side chains (Table 2 and Supplementary Table S1; http://dx.doi.org/10.1667/RR15288.1.S1). Peroxidation (+32) was also observed on a small subset of tripeptides. Previously, +32 mass shifts were observed only on short peptides containing Val, Gly, Ala and Pro (*24*). Furthermore, no peroxidation was observed on basic residues within longer peptides in a second study (*21*). We hypothesize that the differences between tripeptides and longer or more complex peptides can be attributed to a larger variety of chemistries, in addition to variables associated with buffer, radiation source and treatment conditions.

A precise mass shift of –105.042 was identified on GEG, GAG, GNG and GQG (Supplementary Table S1; http://dx.doi.org/10.1667/RR15288.1.S1). Using exact mass calculations, this most likely reflects a loss of $C_3H_7NO_3$ (*54*). The best described phenomenon with a comparable mass change is a radical reaction beginning at the α-carbon of the middle residue (*13, 14, 17, 31, 40*), followed by subsequent cleavage of the C-terminal Gly residue and further decarboxylation. However, this leaves a loss of two hydrogen atoms unaccounted for. A similar mass shift (–104.056) was seen on GPG, which we hypothesize is a related product (Supplementary Table S1; http://dx.doi.org/10.1667/RR15288.1.S1), but small mass discrepancies indicate that more work is required to confirm or update this reaction assignment.

Modifications to Polar and Nonpolar Residues in Tripeptides

Consistent with our observations of a –2 mass shift on the free amino acid Ser, previously observed on free amino acids upon radiolysis (*16*), GSG and GTG both yielded the –2 carbonylation product. A mass shift of –16 was also observed on GSG, which has been previously seen elsewhere (*16*). We hypothesize that this is a loss of oxygen and thus, conversion of the middle residue from Ser to Ala.

Both GNG and GTG, residues containing polar side groups, had exact mass shifts of –48.021, a calculated loss of CH_4O_2 (*54*). This could correspond to radical-mediated decarboxylation of the C-terminus (–30; Fig. 3D), followed by oxygen loss to ultimately result in a C-terminal methyl group, although a further mass shift of –2 is unaccounted for. A mass shift of –4 was seen on the nonpolar residue-containing tripeptides GIG, GLG and GVG. The small mass discrepancies here again indicate that more work is needed to confirm or update the suggested chemistries.

An exact mass shift of –87.03 was observed on the tripeptide GPG (Supplementary Table S1; http://dx.doi.org/10.1667/RR15288.1.S1 and Fig. S10), which corresponds to a net loss of $C_3H_5NO_2$ (*54*). This very likely corresponds

to backbone cleavage and loss of all the atoms C-terminal to the Pro ring, via oxidation of the tripeptide to the 2-pyrrolidone derivative. Backbone cleavage via oxidation of Pro residues has been observed previously elsewhere (*42, 55*), and a mechanism has been defined (*56*). In this case, such cleavage would result in a mass shift of –86, leaving a hydrogen loss unaccounted for and the need for future experiments to confirm this possible similar product.

Modifications to Sulfur-Containing Residues in Tripeptides

Cys has been reported to dimerize to form cystine upon radiolysis via: 1. Thiyl radical formation and reaction with oxygen; 2. Hydroxylated or peroxylated side chain combination via loss of an H_2O_2; or 3. Direct combination of thiyl radicals in conditions lacking oxygen (*46, 47, 57–59*). Consistent with this, we observed a strong signal at m/z 235.06, corresponding to +2 form of the dimerized cystine-containing tripeptide. Although it was present in the control sample, radiolysis strongly induced more cystine formation in a dose-dependent fashion. Concurrent with GCG disulfide dimerization, we identified sulfonic acid (+48) formation, addition of three oxygens to the sulfur atom. These results are consistent with those reported previously by Xu and Chance, in which an identical tripeptide and ^{137}Cs irradiation were used (*60*). In another published study, Xu and Chance identified more oxidative modifications on GCG using MS in negative-mode; specifically, mass shifts of –16, –34, +32, +46, +64 and +80 (*16*). We posit that these modifications were not observed in the current study due to our use of only positive-mode MS analysis for the tripeptides, given that a secondary positive-mode MS analysis in the same publication identified only the –16 mass shift and cystine product formation (*16*).

The tripeptide GMG was highly modified (Table 2 and Supplementary Table S1; http://dx.doi.org/10.1667/RR15288.1.S1). Mass shifts of +16, –14, –32, and –50 were observed. The sulfoxide product, +16, was by far the strongest signal (Supplementary Table S1). The –32 and –14 mass shifts were identified in the previous study by Xu and Chance in which GMG and ^{137}Cs were used (*16*). The –14 product corresponds to decarboxylation (–30) followed by oxidation (+16). The –32 product results from loss of a methanesulfinyl group followed by aldehyde formation at the gamma carbon (*16*). Exact mass measurements using high-resolution MS confirm that the mass shift of –32.008 corresponds precisely to this structural difference. Despite the reactivity of GMG, decarboxylation of the C-terminus was not identified. This is likely due to the strong formation of the –14 product, for which the decarboxylation is a reaction intermediate. Finally, a product with a mass shift of –50.019 was identified (Supplementary Table S3; http://dx.doi.org/10.1667/RR15288.1.S3), which has not been reported before. Reported elemental composition for this mass shift is CH_6S (*54*), which we propose is a loss of these atoms from the Met side chain.

Modifications to Aromatic Residues in Tripeptides

On GYG and GFG, only hydroxylation (+16) and decarboxylation (–30) were identified (Table 2). The tripeptide GWG could only be solubilized in 100% dimethyl sulfoxide (DMSO) due to its strong hydrophobicity. When diluted in dH_2O to a working concentration of 50 μM, this resulted in 0.8% DMSO being present during irradiation. To benchmark possible DMSO-dependent differences in response rate, GIG and GTG were also irradiated in 0.8% DMSO and the response curves were compared to their respective curves without DMSO (Supplementary Table S4; http://dx.doi.org/10.1667/RR15288.1.S4 and Fig. S7; http://dx.doi.org/10.1667/RR15288.1.S5). Under these conditions, GIG and GTG were similar in reactivity rate to their rate without added DMSO. DMSO can modify Trp to form 2-hydroxy-Trp in the presence of HCl as well as DMSO (*61*). With these caveats in mind, the sensitivity of GWG in DMSO was much greater than that of the remaining tripeptides. Signal was lost at 200 Gy irradiation, a result more similar to the more highly-reactive free amino acids than to the tripeptides (Table 2, Supplementary Table S1; http://dx.doi.org/10.1667/RR15288.1.S1 and Fig. S7). Mass shifts of +16n were identified on GWG, up to n = 3, similar to that observed on free Trp. These likely include the products hydroxytryptophan (+16), dihydroxytryptophan (+32) and N-formylkynurenine (+32) (*34, 48*). Two unique products were identified on GWG: mass shifts of +62 and +82. We hypothesize that +62 is a result of four +16n oxidative events concurrent with carbon-carbon double-bond formation somewhere in the molecule (–2). In contrast, +82 may correspond to a product in which there are five +16 events in total as well as hydrogen atom addition across a double bond (+2). Xu and Chance also identified mass shifts of +16n up to n = 5 when the tripeptide GWG underwent radiolysis (*17*). Our identification of +16n mass shifts (with minor adducts or losses) up to n = 5 here corroborates this data. In general, our data highlight the fact that one must pay attention to all chemical species present in the mixture when irradiation is performed, as even small amounts of solvents or buffers may make a large difference in the results obtained.

CONCLUSIONS

We have begun to study, in a methodical fashion, the effect of Linac-produced radiation on amino acids and tripeptides, with the goal of elucidating the differences between simplified systems and systems of more complexity when exposed to ionizing radiation. The ultimate goal was to infer testable biological implications from datasets such as that produced here. However, there is a need for fundamental groundwork as the basis for future studies. In this study, novel mass shifts were observed. In contrast, modifications observed in previously published studies

were not seen here. The results described herein underscore the notion that radiosensitivity of amino acids is highly contextual. Incorporating amino acids into a simple tripeptide substantially reduces their sensitivities, a result observed here as well as in comparisons of these data to many other studies. Additionally, modification patterns obtained by exposing free amino acids to radiation may not readily be extrapolated to irradiation of the same amino acid residues within peptides. This claim is supported by both quantitative (dose-response rates) and qualitative (chemical modifications) variability observed between even the simple systems used in these experiments. Furthermore, variability in amino acid response is also evident when comparing published studies, likely due to differences in solution conditions, radiation source or the exact amino acid sequence of the peptides used. Future studies will be undertaken to further examine these differences, and elucidate the effect of radiation on biological molecules in highly controlled and reproducible conditions. Overall, the results begin to provide a basis for identifying radiation-related protein damage on a proteomic scale.

SUPPLEMENTARY INFORMATION

Table S1. Tripeptide radiation sensitivity and modification patterns, collected using electrospray ionization-orbitrap mass spectrometry. Each tripeptide is shown on a different sheet. Charts are extracted ion chromatograms for the specified species for each dosage, used for the quantification tables shown below them. The extracted mass is displayed above the respective table per species. The data here were used to build the charts for Supplementary Figs. S8–10. All masses displayed are m/z (Da/charge state).

Table S2. Free amino acid radiosensitivity and modification patterns, collected using electrospray ionization-time of flight mass spectrometry. Each amino acid is shown both for positive and negative mode on individual sheets. Below are the automatically extracted masses, their retention times, peak heights, and identified adducts. Above, values for quantification were built on extracted ion chromatograms of the specified masses (the example of the unmodified is given in every case). In many cases, shown in bolded red, the automatic peak picking informed the masses to manually extract. Masses that were extracted and quantified above but not bolded in red below were chosen based on literature reports, cited in the main text. The data here were used to build charts for Supplementary Figs. S1–S3. All masses displayed are m/z (Da/charge state), though charge states of only +1 or –1 were observed.

Table S3. Data used for low abundance tripeptides, including GQG, GDG, GPG and GKG. Each was tested by concentration from stock exposure 2×, 5× and 10×. For all of these, the tenfold concentration was used as representative, and the data from those exposures are used in Figs. 3A–C. All masses displayed are m/z (Da/charge state).

Table S4. Data used for tripeptides in DMSO figure. Each of the three tripeptides is shown on a separate sheet.

Figs. S1–S3. Product formation over a range of 0–1,000 Gy for the free amino acids. Known modifications are shown as atomic adducts, whereas unknown modifications are shown as mass shifts. The y-axes are unitless, and are raw signal intensities for the listed modifications.

Fig. S4. Clustering and ESI-TOF data demonstrating sensitivities of nonpolar, polar, charged and aromatic free amino acids.

Fig. S5. Correlations of sensitivities (slope over linear range of signal loss for unmodified versions, all x-axes) with physicochemical properties for free amino acids.

Fig. S6. Reproducibility of experiments. Top left: Three technical replicates (same sample, analyzed thrice with same instrumental method, processing, etc. postirradiation) of GKG at low concentration. Top right and bottom: Experimental replicates (samples independently made up, exposed and analyzed). Top right: GMG twice independently diluted to 50 μ*M*, irradiated and analyzed, approximately one month apart. Bottom left: GVG twice independently diluted to 50 μ*M*, irradiated and analyzed, approximately one month apart.

Fig. S7. Comparison of sensitivity for two tripeptides in dH_2O and 0.8% DMSO. All tripeptides are 50 μ*M*.

Figs. S8–S10. Product formation over a range of 0–1,000 Gy for the tripeptides. Known modifications are shown as atomic adducts, whereas unknown modifications are shown as mass shifts. The y-axes are unitless, and are raw signal intensities for the listed modifications.

Fig. S11. Correlations of relative sensitivities (slope over linear range of signal loss for unmodified versions) with physicochemical properties for free amino acids.

ACKNOWLEDGMENTS

We gratefully acknowledge funding provided to BBM, GS, STB, MMC and MRS by the U.S. Department of Defense (Homeland DTRA grant no. HDTRA1-16-1-0049) and to STB and MMC by the National Institutes of Health (NIH grant no. GM112575). Funding was also provided to STB by the Morgridge Biotechnology Fellowship from the Vice Chancellor's Office for Research and Graduate Education and the UW Biotechnology Center.

Received: November 12, 2018; accepted: February 13, 2019; published online: March 8, 2019

REFERENCES

1. Daly MJ. A new perspective on radiation resistance based on Deinococcus radiodurans. Nat Rev Microbiol 2009; 7:237–45.
2. Krisko A, Radman M. Biology of extreme radiation resistance: the way of Deinococcus radiodurans. Cold Spring Harb Perspect Biol 2013; 5.
3. Morgan MA, Lawrence TS. Molecular pathways: overcoming radiation resistance by targeting DNA damage response pathways. Clin Cancer Res 2015; 21:2898–904.
4. Hashimoto T, Kunieda T. DNA protection protein, a novel mechanism of radiation tolerance: lessons from tardigrades. Life (Basel) 2017; 7.

5. Jung KW, Lim S, Bahn YS. Microbial radiation-resistance mechanisms. J Microbiol 2017; 55:499–507.
6. Ranawat P, Rawat S. Radiation resistance in thermophiles: mechanisms and applications. World J Microbiol Biotechnol 2017; 33:112.
7. Shuryak I, Matrosova VY, Gaidamakova EK, Tkavc R, Grichenko O, Klimenkova P, et al. Microbial cells can cooperate to resist high-level chronic ionizing radiation. PLoS One 2017; 12:e0189261.
8. Jung KW, Yang DH, Kim MK, Seo HS, Lim S, Bahn YS. Unraveling fungal radiation resistance regulatory networks through the genome-wide transcriptome and genetic analyses of cryptococcus neoformans. MBio 2016; 7.
9. Anno GH, Young RW, Bloom RM, Mercier JR. Dose response relationships for acute ionizing-radiation lethality. Health Phys 2003; 84:565–75.
10. Islam MT. Radiation interactions with biological systems. Int J Radiat Biol 2017; 93:487–93.
11. Davies MJ. The oxidative environment and protein damage. Biochim Biophys Acta 2005; 1703:93–109.
12. Davies MJ. Reactive species formed on proteins exposed to singlet oxygen. Photochem Photobiol Sci 2004; 3:17–25.
13. Davies KJ, Delsignore ME, Lin SW. Protein damage and degradation by oxygen radicals. II. Modification of amino acids. J Biol Chem 1987; 262:9902–7.
14. Stadtman ER. Oxidation of free amino acids and amino acid residues in proteins by radiolysis and by metal-catalyzed reactions. Annu Rev Biochem 1993; 62:797–821.
15. Stadtman ER, Levine RL. Free radical-mediated oxidation of free amino acids and amino acid residues in proteins. Amino Acids 2003; 25:207–18.
16. Xu G, Chance MR. Radiolytic modification of sulfur-containing amino acid residues in model peptides: fundamental studies for protein footprinting. Anal Chem 2005; 77:2437–49.
17. Xu G, Chance MR. Hydroxyl radical-mediated modification of proteins as probes for structural proteomics. Chem Rev 2007; 107:3514–43.
18. Benon H.J. Bielski DEC, Alberta B. Ross, Ravindra L. Arudi. Reactivity of HO2/O–2 radicals in aqueous solution. J Phys Chem Ref Data 1985; 14:1041–100.
19. George V. Buxton CLG, W. Phillips Helman, Alberta B. Ross. Critical review of rate constants for reactions of hydrated electrons, hydrogen atoms and hydroxyl radicals ($^{\bullet}$OH/$^{\bullet}$O–) in aqueous solution. J Phys Chem Ref Data 1988; 17:513–886.
20. Kaur P, Kiselar JG, Chance MR. Integrated algorithms for high-throughput examination of covalently labeled biomolecules by structural mass spectrometry. Anal Chem 2009; 81:8141–9.
21. Xu G, Takamoto K, Chance MR. Radiolytic modification of basic amino acid residues in peptides: probes for examining protein-protein interactions. Anal Chem 2003; 75:6995–7007.
22. Xu G, Chance MR. Radiolytic modification of acidic amino acid residues in peptides: probes for examining protein-protein interactions. Anal Chem 2004; 76:1213–21.
23. Saladino J, Liu M, Live D, Sharp JS. Aliphatic peptidyl hydroperoxides as a source of secondary oxidation in hydroxyl radical protein footprinting. J Am Soc Mass Spectrom 2009; 20:1123–6.
24. Morgan PE, Pattison DI, Davies MJ. Quantification of hydroxyl radical-derived oxidation products in peptides containing glycine, alanine, valine, and proline. Free Radic Biol Med 2012; 52:328–39.
25. De Meutter P, Camps J, Delcloo A, Termonia P. Source localisation and its uncertainty quantification after the third DPRK nuclear test. Sci Rep 2018; 8:10155.
26. Williams M, Sizemore DC. Biologic, chemical, and radiation terrorism review. Treasure Island, FL: StatPearls; 2018.
27. Jorgensen TJ. Predicting the public health consequences of a nuclear terrorism attack: drawing on the experiences of Hiroshima and Fukushima. Health Phys 2018; 115:121–5.
28. Smirnova OA, Cucinotta FA. Dynamical modeling approach to risk assessment for radiogenic leukemia among astronauts engaged in interplanetary space missions. Life Sci Space Res (Amst) 2018; 16:76–83.
29. Jandial R, Hoshide R, Waters JD, Limoli CL. Space-brain: The negative effects of space exposure on the central nervous system. Surg Neurol Int 2018; 9:9.
30. Bruckbauer ST, Trimarco JD, Martin J, Senn KA, Schackwitz W, Lipzen A, et al. Experimental evolution of extreme resistance to ionizing radiation in Escherichia coli after 50 cycles of selection. J Bacteriol 2019. (DOI: 10.1128/JB.00784-18)
31. Davies MJ, Dean RT. Radical-mediated protein oxidation. New York: Oxford University Press; 1997.
32. Zamyatnin AA. Protein volume in solution. Prog Biophys Mol Biol 1972; 24:107–23.
33. Kyte J, Doolittle RF. A simple method for displaying the hydropathic character of a protein. J Mol Biol 1982; 157:105–32.
34. Finley EL, Dillon J, Crouch RK, Schey KL. Identification of tryptophan oxidation products in bovine a-crystallin. Protein Sci 1998; 7:2391–7.
35. Heinecke JW, Li W, Daehnke HL 3rd, Goldstein JA. Dityrosine, a specific marker of oxidation, is synthesized by the myeloperoxidase-hydrogen peroxide system of human neutrophils and macrophages. J Biol Chem 1993; 268:4069–77.
36. Huggins TG, Wells-Knecht MC, Detorie NA, Baynes JW, Thorpe SR. Formation of o-tyrosine and dityrosine in proteins during radiolytic and metal-catalyzed oxidation. J Biol Chem 1993; 268:12341–7.
37. Marquez LA, Dunford HB. Kinetics of oxidation of tyrosine and dityrosine by myeloperoxidase compounds I and II. Implications for lipoprotein peroxidation studies. J Biol Chem 1995; 270:30434–40.
38. Maskos Z, Rush JD, Koppenol WH. The hydroxylation of phenylalanine and tyrosine: a comparison with salicylate and tryptophan. Arch Biochem Biophys 1992; 296:521–9.
39. Easton CJ. Free-radical reactions in the synthesis of alpha-amino acids and derivatives. Chem Rev 1997; 97:53–82.
40. Garrison WM. Reaction mechanisms in the radiolysis of peptides, polypeptides, and proteins. Chem Rev 1987; 87:381–98.
41. Amici A, Levine RL, Tsai L, Stadtman ER. Conversion of amino acid residues in proteins and amino acid homopolymers to carbonyl derivatives by metal-catalyzed oxidation reactions. J Biol Chem 1989; 264:3341–6.
42. Dean RT, Wolff SP, McElligott MA. Histidine and proline are important sites of free radical damage to proteins. Free Radic Res Commun 1989; 7:97–103.
43. Requena JR, Chao CC, Levine RL, Stadtman ER. Glutamic and aminoadipic semialdehydes are the main carbonyl products of metal-catalyzed oxidation of proteins. Proc Natl Acad Sci U S A 2001; 98:69–74.
44. Li S, Schoneich C, Borchardt RT. Chemical pathways of peptide degradation. VIII. Oxidation of methionine in small model peptides by prooxidant/transition metal ion systems: influence of selective scavengers for reactive oxygen intermediates. Pharm Res 1995; 12:348–55.
45. Vogt W. Oxidation of methionyl residues in proteins: tools, targets, and reversal. Free Radic Biol Med 1995; 18:93–105.
46. Armstrong DA. Applications of pulse radiolysis for the study of short-lived sulphur species. In: Chatgilialoglu C, Asmus, K-D, editors. Sulfur-centered reactive intermediates in chemistry and biology. New York: Plenum Press; 1990. p. 121–34.
47. von Sonntag C. Free-radical reactions involving thiols and disulphides. In: Chatgilialoglu C, Asmus, K-D, editors. Sulfur-

centered reactive intermediates in chemistry and biology. New York: Plenum Press; 1990. p. 359–66.

48. Stadtman ER. Role of oxidized amino acids in protein breakdown and stability. In: Klinman JP, editor. Methods in enzymology. Redox-active amino acids in biology, Volume 258. Elsevier; 1995.

49. Hawkins CL, Davies, M.J. Generation and propagation of radical reactions on proteins. Biochim Biophys Acta 2001; 1504:196–219.

50. Uchida K, Kawakishi S. Selective oxidation of imidazole ring in histidine residues by the ascorbic acid-copper ion system. Biochem Biophys Res Commun 1986; 138:659–65.

51. Rao PS, Simic, M., Hayon, E. Pulse radiolysis study of imidazole and histidine in water. J Phys Chem 1975; 79.

52. Tomita M, Masachika I, Tyunosin U. Sensitized photooxidation of histidine and its derivatives. Products and mechanism of the reaction. Biochemistry 1969; 8:5149–60.

53. Harpaz Y, Gerstein M, Chothia C. Volume changes on protein folding. Structure 1994; 2:641–9.

54. Patiny L, Borel A. ChemCalc: a building block for tomorrow's chemical infrastructure. J Chem Inf Model 2013; 53:1223–8.

55. Schuessler H, Schilling K. Oxygen effect in the radiolysis of proteins. Part 2. Bovine serum albumin. Int J Radiat Biol Relat Stud Phys Chem Med 1984; 45:267–81.

56. Uchida K, Kato Y, Kawakishi S. A novel mechanism for oxidative cleavage of prolyl peptides induced by the hydroxyl radical. Biochem Biophys Res Commun 1990; 169:265–71.

57. Lal M. Radiation induced oxidation of sulphydryl molecules in aqueous solutions. A comprehensive review. Radiat Phys Chem 1994; 43:595–611.

58. Dewey DL, Beecher J. Interconversion of cystine and cysteine induced by x-rays. Nature 1965; 206:1369–70.

59. Owen TC, Brown MT. Radiolytic oxidation of cysteine. J Org Chem 1969; 34:1161–2.

60. Xu G, Chance MR. Radiolytic modification and reactivity of amino acid residues serving as structural probes for protein footprinting. Anal Chem 2005; 77:4549–55.

61. Savige WE, Fontana A. Oxidation of tryptophan to oxindolylalanine by dimethyl sulfoxide-hydrochloric acid. Selective modification of tryptophan containing peptides. Int J Pept Protein Res 1980; 15:285–97.

62. Almond PR, Biggs PJ, Coursey BM, Hanson WF, Huq MS, Nath R, et al. AAPM's TG-51 protocol for clinical reference dosimetry of high-energy photon and electron beams. Med Phys 1999; 26:1847–70.